

Developing a tool based on weather radar to assess mass spruce budworm moth flights during an outbreak

A demonstration of the capability of weather radars to monitor the flight of spruce budworm moth flights around the Gulf of the St-Lawrence River

Frédéric Fabry and Alamelu Kilambi, McGill University

Context: Weather radars and insects

Weather radars

All over North America and elsewhere around the world, radars have been installed and are being used to monitor the weather (Fig. 1). This infrastructure was installed over the years to detect severe weather and warn people and authorities in case of meteorological threats. In Canada, 31 radars are used specifically for this *weather surveillance*, mostly covering the south of the country.

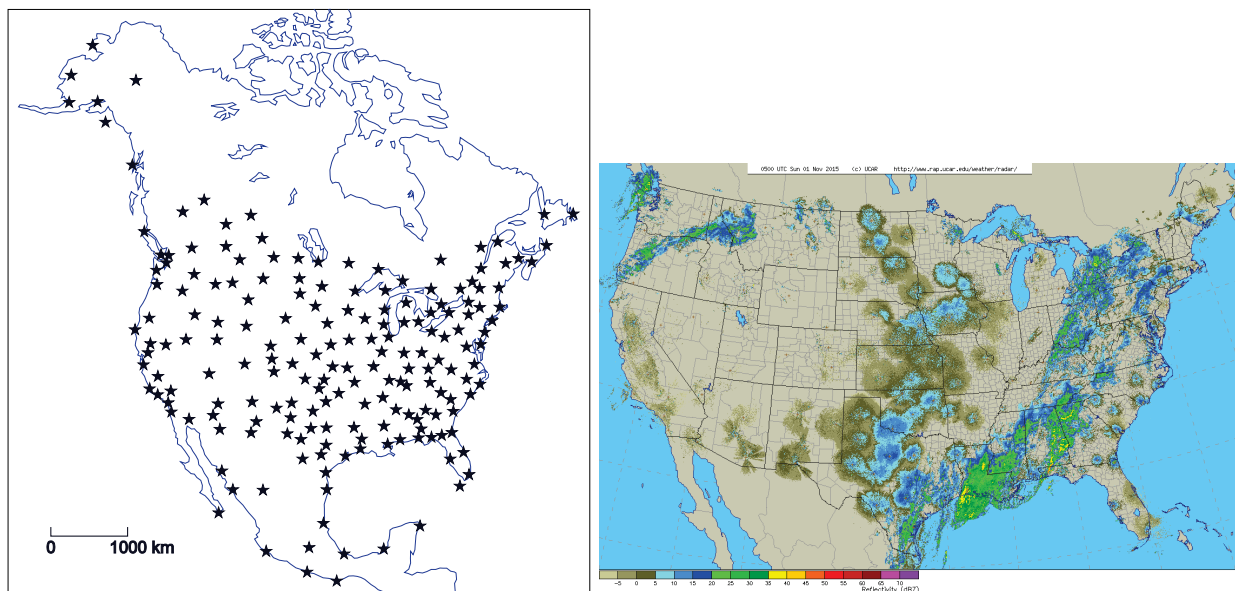


Fig. 1: Left: North American network of weather radars circa 2015 (Fabry 2015). Not included in this figure are weather radars dedicated for airport terminal use and those owned by non-governmental organizations such as TV stations. Right: Example of the echoes observed by these radars over the United States at 0:00 EST on 1 November 2015. Stronger echoes in blue and green patches in the East and North West are from precipitation, while weaker echoes in gray and cyan in the middle of the continent are from migrating birds. Image courtesy of the National Center for Atmospheric Research (© 2015).

Radar and its targets

Radar get their information by sending a short high-power microwave pulse (think of it as a scream) and listening to the characteristics of the echoes of that pulse reflected by objects known as *targets* (recall that radar was first developed for military applications). Though weather radars have been designed and optimized to detect weather, many objects can reflect microwave pulses and hence be detected by radar: cars (got a ticket lately?), boats, airplanes, rain, snow, hail and other hydrometeors (“water-made objects falling from the sky”), the ground and sea surfaces, and finally biological targets such as birds and insects. Each target will reflect a different amount of energy based on its size, shape, and the material it is made of. The intensity of the echo is hence our first clue in determining what type of target we are dealing with. The target may be moving or stationary, isolated or part of a cluster whose echo has a specific spatial texture, extend vertically or not; the accumulation of the characteristics observed on radar display is then used to determine the type of target observed, or at least narrow it down to a limited set of possibilities (see Appendix A for additional details). For example, while precipitation and insects echoes have similar extent on radar displays and both move more or less with the wind, they can be distinguished using the altitude up to which the echoes are observed, rain originating generally from heights above 3 km while insects rarely reach that level. Insect and precipitation echoes also have somewhat different intensities (Table 1) as well as texture that also help in their identification.

Table 1. Typical values of observed radar reflectivity factors from different targets (Fabry 2015)

Target type	Z_e
Light drizzle; insects	0 dBZ
Moderate drizzle; a few raindrops; light snow; migrating birds	10 dBZ
Light rain or moderate snow, typical of widespread precipitation (1 mm/hr)	25 dBZ
Moderate precipitation, strong for widespread precipitation (5 mm/hr)	35 dBZ
Heavy rain from a convective shower (20 mm/hr)	45 dBZ
Hail or very heavy rain, peak of thunderstorms (100+ mm/hr)	55 dBZ
Hail	>60 dBZ

Once the nature of the target is known, knowledge of the expected size and characteristics of the target observed can then be used to estimate their number density. For example, a typical female spruce budworm (SBW) moth weighing of the order of 12 mg (Thomas et al. 1980) per km^3 should have a reflectivity of the order of -58 dBZ. This information then gives us a way estimate moth number density from the echo strength measured by radar (see Appendix B for details on this estimation).

That being said, ambiguities remain because of the large variety of targets observed by weather radars. Insects in general can be distinguished, but one must rely on external information in order to determine what types of insects dominate the signal. In the case of the Val d'Irène radar, waves on the surface of the water from the Gulf of St-Lawrence, generally known as sea clutter, will be observed in windy conditions and have an appearance on radar that is difficult to distinguish from that of insects. Finally,

very strong targets from the ground surface, referred to as ground clutter, will often mask the much weaker echoes of insects. The proper use of radar for insect detection and quantification hence demands a fair bit of work to minimize those ambiguities, accepting the fact that, in the end, some of those will remain.

Measurements of weather surveillance radars and their scanning strategy

Radar used for the real-time monitoring of weather share particular characteristics to help them achieve their task. They first generally function at frequencies where precipitation can both be observed and yet does not affect radar performance significantly. This is best achieved at wavelengths of the order of 5 cm (used by all Environment Canada radars) or 10 cm (used by McGill and in the United States). They also measure characteristics that help us identify the type of (weather) target observed. This includes reflectivity, related to the number and size of raindrops or snowflakes per unit volume, the Doppler velocity, or whether the target appears to be moving towards or away from the radar, and increasingly dual-polarization information, providing some clues about target shapes. In Canada, only the King City (Toronto) and McGill (Montreal) radar have dual-polarization capability, though this is expected to change in a few years.

To help detect possible threats from weather, it is essential to measure weather echoes at different altitudes all around the radar, and make periodic revisit to monitor the possibly rapid evolution of severe weather. This need shapes what is known as the scanning strategy of weather radars. For maximum coverage in short times, scanning in azimuth (or “horizontally”) remains the best approach. These basic scans are known for historical reasons as PPIs. To monitor the weather around the radar at multiple altitudes, several of these PPIs are made at different elevation angles (Fig. 2). In Canada, it is common to use 24 elevation angles completed in five minutes to get a good picture of the weather around a radar (Fig. 2). But because these fast scans are not ideal to measure velocity or to clean ground targets, another set of four slow-scan PPIs are often added for better measuring velocity and better get rid of stationary ground targets. All Canadian radars except the McGill system hence use a 10-min volume scan: The first five minutes are used for scans that measure reflectivity at 24 elevation angles at the risk of having it contaminated by ground targets (these scans are known as “ConVol” in the Canadian weather radar jargon); the next five minutes are then used to make four PPIs with a much reduced antenna rotation velocity to get better velocity measurement and to be able to filter ground targets for those scans (“DopVol” in the Canadian weather radar jargon).

This scanning strategy shapes what data are available for insect monitoring. Every 10 minutes, we obtain reflectivity information at many angles of the ConVol, but that information may be contaminated by ground targets. Then we have information the DopVol information that is cleaned from ground targets, but only available at a few elevation angles and that also has a bit less sensitivity than the ConVol scans. Our analysis of insect coverage and dispersal will hence use a combination of the more sensitive and higher coverage ConVol scans blended with the cleaned DopVol scans.

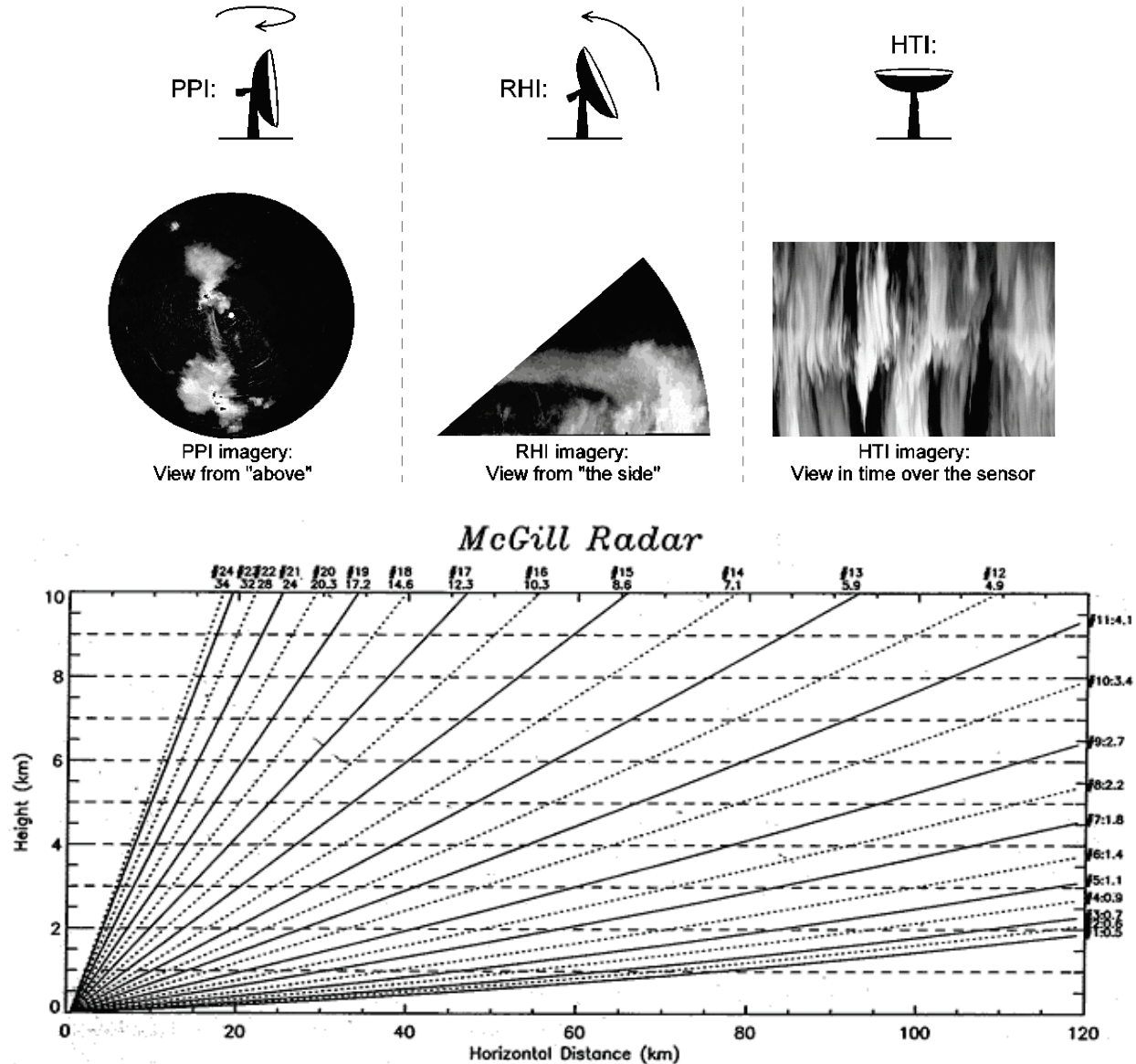


Fig. 2: Top: Illustration of basic weather radar scans: PPIs (or scans in azimuth at a constant elevation), RHIs (or scans in elevation at a constant azimuth), and HTIs (stares in the vertical). Weather surveillance radars use primarily PPIs, or scans in azimuth at a constant elevation angle above (or below) the horizon. Bottom: Set of elevation angles that constitutes a radar volume scan, here for the McGill Radar.

With this brief introduction to weather radars completed, we now attack the presentation of the research work itself.

Weather radar and SBW moths: Capability demonstration

As part of research funded by the Forestry Service of Natural Resources Canada, we were initially tasked to do the following:

- Thoroughly analyze and interpret radar echoes of the July 15-16th 2013 from the Val d'Irene radar;
- Develop an approach to characterize the spatiotemporal patterns (initiation, direction, relative density) of the mass flight observed on the night of July 15-16th 2013 over the North Shore and the Lower St. Lawrence region;
- Generate maps (rasters) of echo strength (corrected for topography) at different elevation angles for ten selected nights of July 2013 where significant insect echoes are observed.

The work was undertaken as part of a larger effort seeking to investigate the possibility of using dispersion information to help within early intervention strategy that could help control of the spruce budworm in following years.

We however realized that a proper analysis of the radar data could be better done if a process for obtaining improved imagery was developed. Hence, we replaced the third task by the development of a process, known as a radar product, to obtain better quality insect maps.

Data source and product development

The key data source used in this study is the radar data collected by the Val d'Irene radar (48.48 N, 67.60 W) of Environment Canada (Fig. 3). At 710 m altitude, the radar covers the eastern Bas Saint-Laurent, western Gaspésie, and the Haute Côte Nord region of the Gulf of St-Lawrence. Figure 3 also shows an example of the data made available by Environment Canada on their web site on the night of 15-16 July 2013. A significant fraction of the echoes observed in cyan and light green is seen moving from the North Shore towards the South Shore, and is believed to be coming from dispersing SBW moths.

Observations made by Yan Boulanger of such data triggered the interest of the Canadian Forest Service and was the genesis of this work. The reflectivity image in Fig. 3 also illustrates some of the weaknesses in the traditional data processing. First, while ground echoes were eliminated within 120 km using the DopVol data, they remain beyond 120 km, resulting in strong echoes from the ground being observed especially on the North Shore west and north of the radar. Second, at closer range in areas where strong ground echoes were suppressed (just west and north of Baie Comeau for example), all echoes have vanished as strong ground targets masked the much weaker insect echoes. Trying to recover information in these two regions will be one of our main tasks.

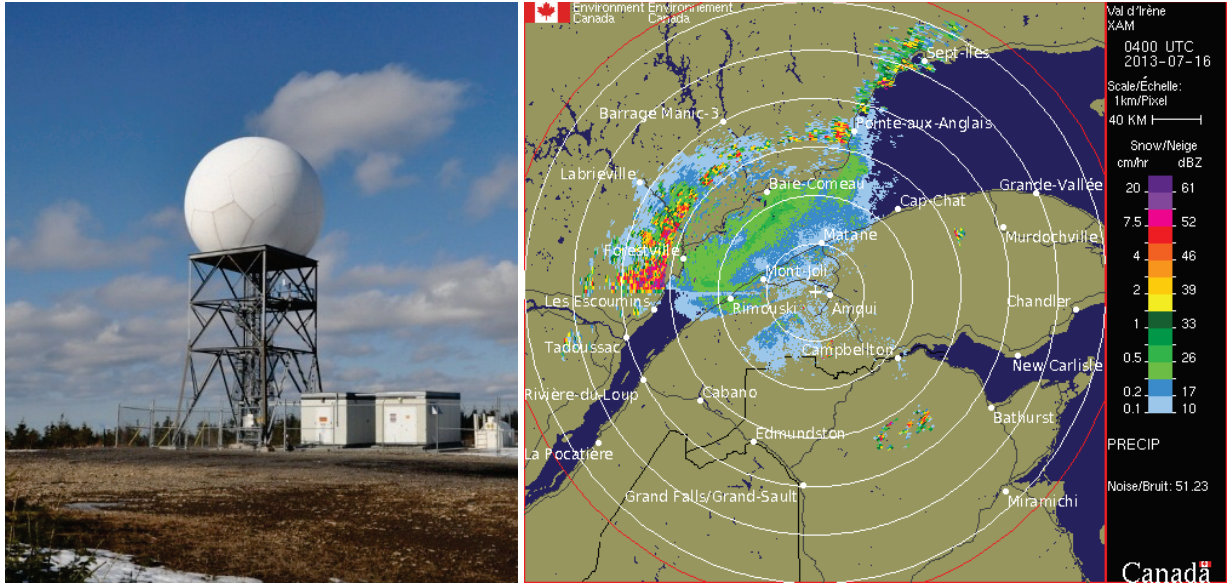


Fig. 3: Left: The Val d'Irène radar used in this study. Right: Radar reflectivity observed by the Val d'Irène radar near the peak of the dispersal (04:00 UTC, or 0:00 EDT) on the night of 15-16 July 2013 as made available on Environment Canada web sites. Images courtesy of Environment Canada.

Our first task was to develop a base product to monitor the horizontal movement of insects. After several different attempts we settled on the following. Data from the five lowest elevation scans of ConVol (-0.5° , -0.3° , -0.1° , 0.1° , and 0.3°) are combined with the data from the low 3 elevation scans of DopVol (long range -0.5° , short range -0.5° , and short range -0.2°), taking advantage of the higher sensitivity of the ConVol scans and the ground clutter removal of the DopVol scans. The product conserves the higher sensitivity of the ConVol scans by taking the maximum reflectivity in the 5 low elevation scans. Then, the clutter pixels in the ConVol scans are identified by an average clutter mask, and replaced by the maximum of 3 lowest DopVol scans. Because insects tend to stay close to the surface, the peak reflectivity among a set of angles is generally from the lowest angle, unless that angle is contaminated by clutter or affected by beam blockage. Finally, high reflectivity values (greater than 25 dBZ) with low echo tops (lower than 2.5 km) over the ground are considered to be unfiltered ground targets and are replaced by an average of the reflectivity values from the immediate neighborhood. The resulting product hence shows the maximum reflectivity observed by radar at low elevations that can be attributed to insects or precipitation. In the case of the night of 15-16 July 2013, no precipitation echo was observed; all the echoes that are not from the ground are from the waves on the Gulf or from insects.

The result of the radar data processing can be seen in Fig. 4. In situations like these where insect dispersal was particularly important, we were successful in retrieving insect echoes in clutter areas (both suppressed and not suppressed) by using information from multiple elevation angles. Blocked sectors, such as WSW of the radar, however remain blocked, and good insect observations are impossible to be made in these sectors.

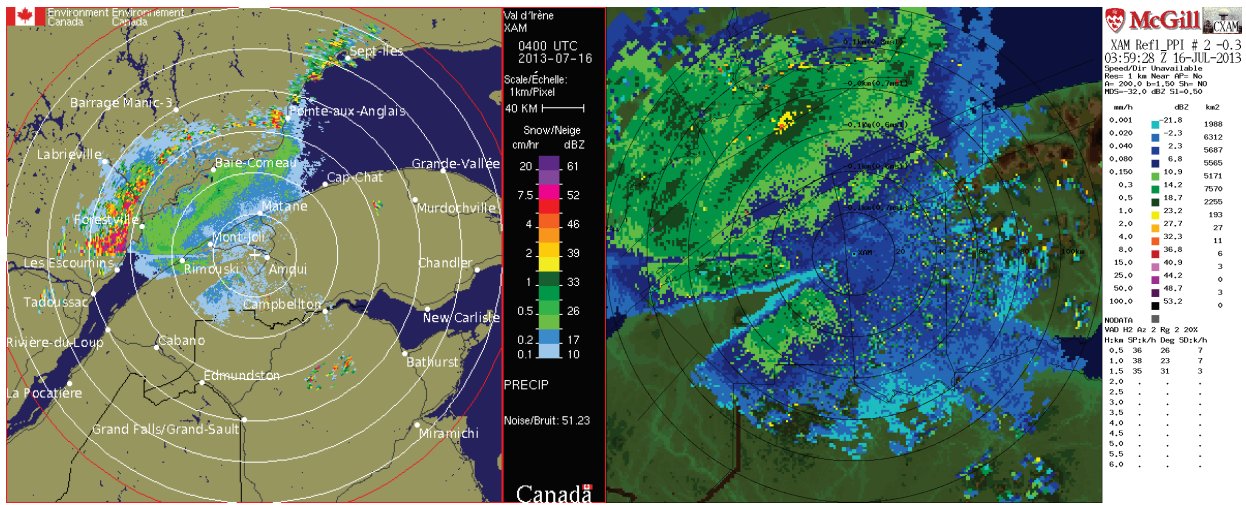
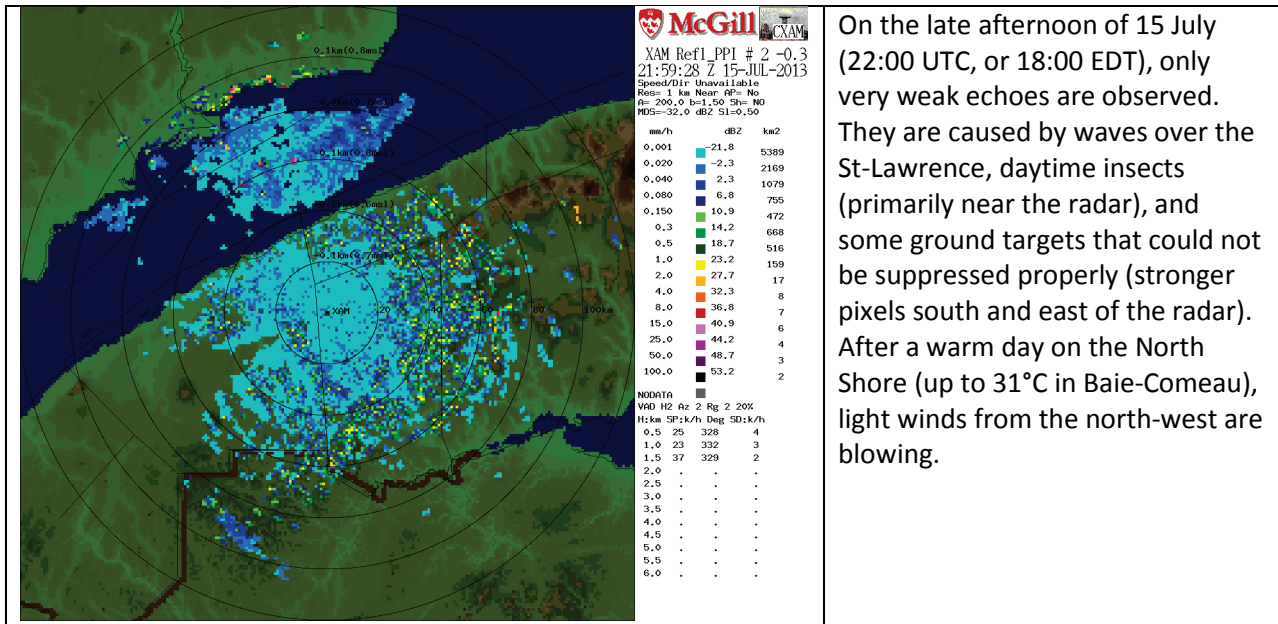


Fig. 4: Illustration of the result of the processing to obtain an insect echo map, contrasting the original image from Environment Canada (left) with the one we derived after combining information from the DopVol and ConVol volume scans (right). Note the different spatial and reflectivity scales when comparing the two images.

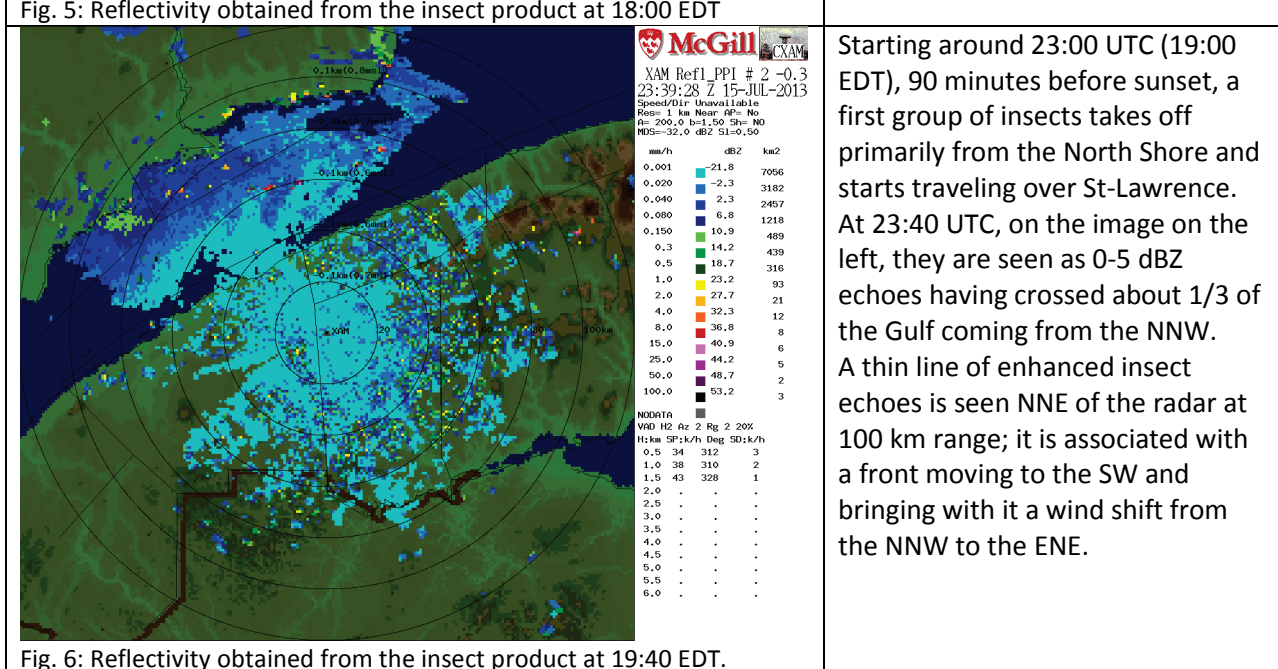
The dispersal of 15-16 July 2013

With the cleaned images at our disposal, we are able to better analyze the sequence of events that occurred on the night of 15-16 July 2013. The night's sequence of events blends in an interesting way meteorology and insect dispersal.

The following sequence of commented images shows the evolution during the evening and over the night of the peak insect reflectivity. These images are available in data and image form every 10 minutes from 21:00 UTC (17:00 EDT) to 10:00 UTC (6:00 EDT), but only a subset of them are shown here.



On the late afternoon of 15 July (22:00 UTC, or 18:00 EDT), only very weak echoes are observed. They are caused by waves over the St-Lawrence, daytime insects (primarily near the radar), and some ground targets that could not be suppressed properly (stronger pixels south and east of the radar). After a warm day on the North Shore (up to 31°C in Baie-Comeau), light winds from the north-west are blowing.



Starting around 23:00 UTC (19:00 EDT), 90 minutes before sunset, a first group of insects takes off primarily from the North Shore and starts traveling over St-Lawrence. At 23:40 UTC, on the image on the left, they are seen as 0-5 dBZ echoes having crossed about 1/3 of the Gulf coming from the NNW. A thin line of enhanced insect echoes is seen NNE of the radar at 100 km range; it is associated with a front moving to the SW and bringing with it a wind shift from the NNW to the ENE.

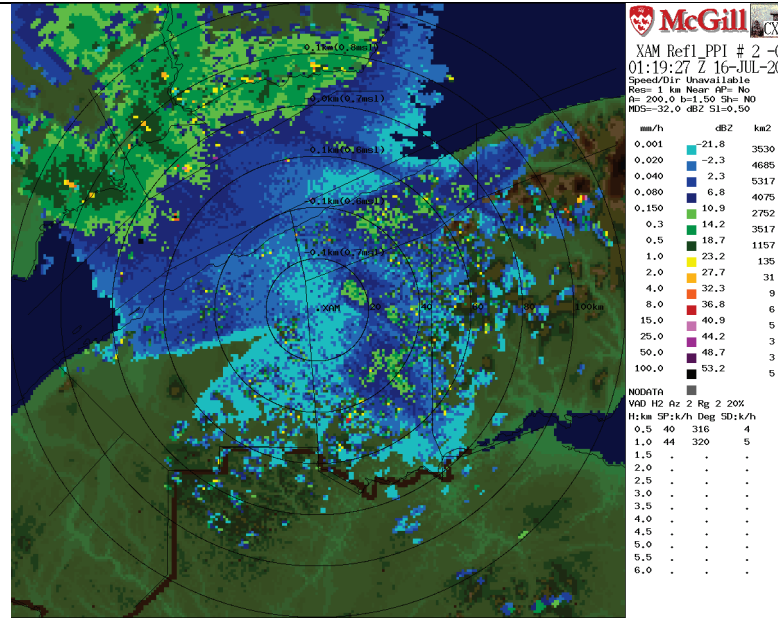


Fig. 7: Reflectivity obtained from the insect product at 21:20 EDT.

It is just after sundown that the main group of insects are taking off, having a reflectivity 30 times stronger than the initial wave. Of the order of 6000 km^2 of insect echoes averaging 20 million moths per km^{-2} (given the $\sim 1 \text{ km}$ beam width at that range) are observed to take off from the North Shore. The first elements of the initial wave have reached the South Shore while the main group is starting its crossing, all moving at about 40 km/hr. Smaller groups are also seen taking off from specific locations in the Gaspésie region that were affected by the SBW.

In parallel, the wind shift line is now 60 km NNE of the radar, with the result that insects behind it are pushed to the SW.

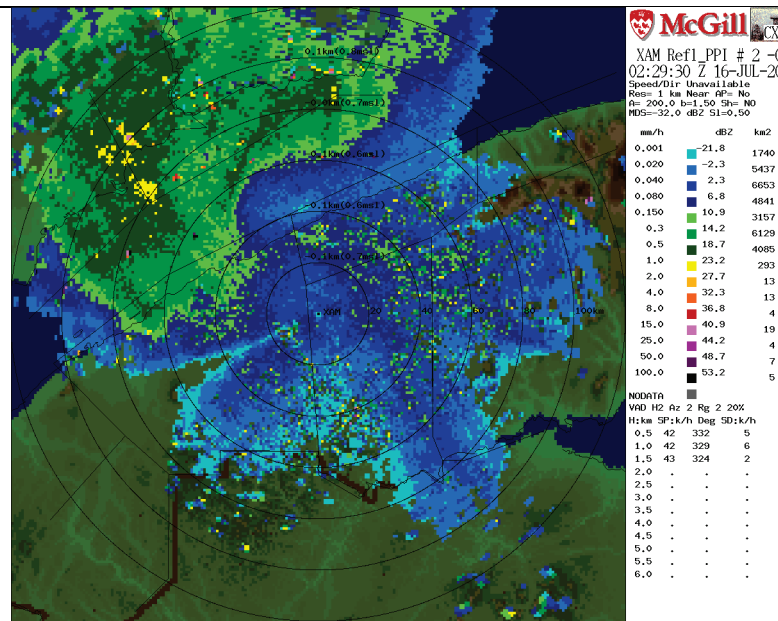


Fig. 8: Reflectivity obtained from the insect product at 22:30 EDT.

02:30 UTC (22:30 EDT): The first elements of the main group have made it over the Gulf, but only well west of Matane. The South Shore east of Matane has been mostly protected by the wind shift that is pushing the insects up the St-Lawrence Valley. The smaller group originating from Gaspésie is moving south, some reaching New Brunswick. Radar coverage being poorer to the south, it is hard to tell if most of them have landed or if they are still flying.

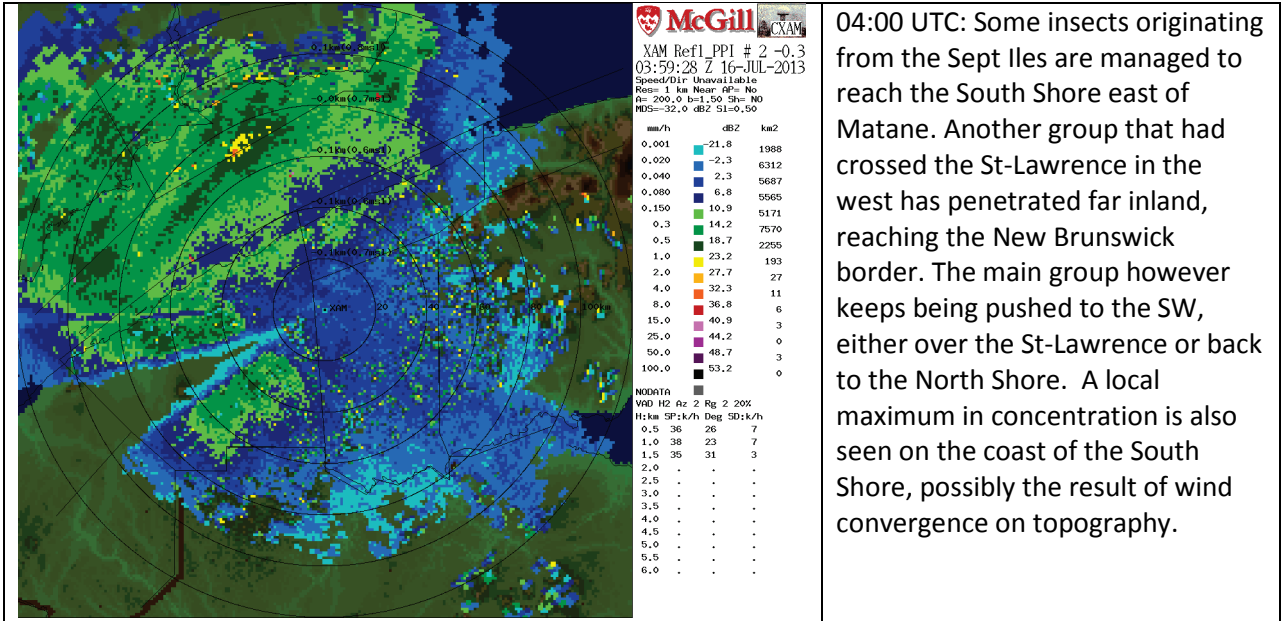


Fig. 9: Reflectivity obtained from the insect product at 0:00 EDT.

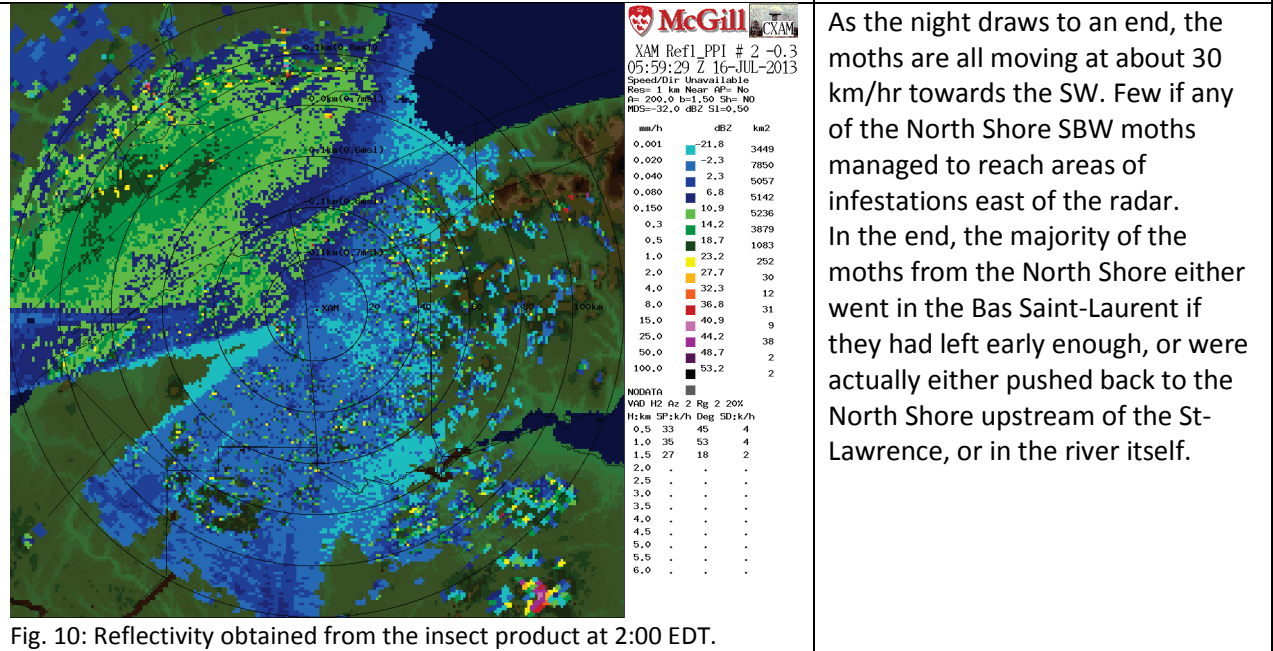


Fig. 10: Reflectivity obtained from the insect product at 2:00 EDT.

Vertical sections made over the river where ground echo contamination is minimized (Fig. 11) show that insect echoes are primarily concentrated below 500 m altitude. The exact vertical distribution of insects remains unknown because 1) the number of PPI scans made by the radar is insufficient at low levels and 2) the echoes are smoothed by the 0.65° beam of the radar that smooth patterns in the vertical over 500 m at 40-50 km range of the radar. Note that such a shallow echo is in sharp contrast with most precipitation echoes: except for drizzle, rain echoes, especially in summer, extend vertically at least up to 6 km altitude, making them easy to distinguish from insect echoes.

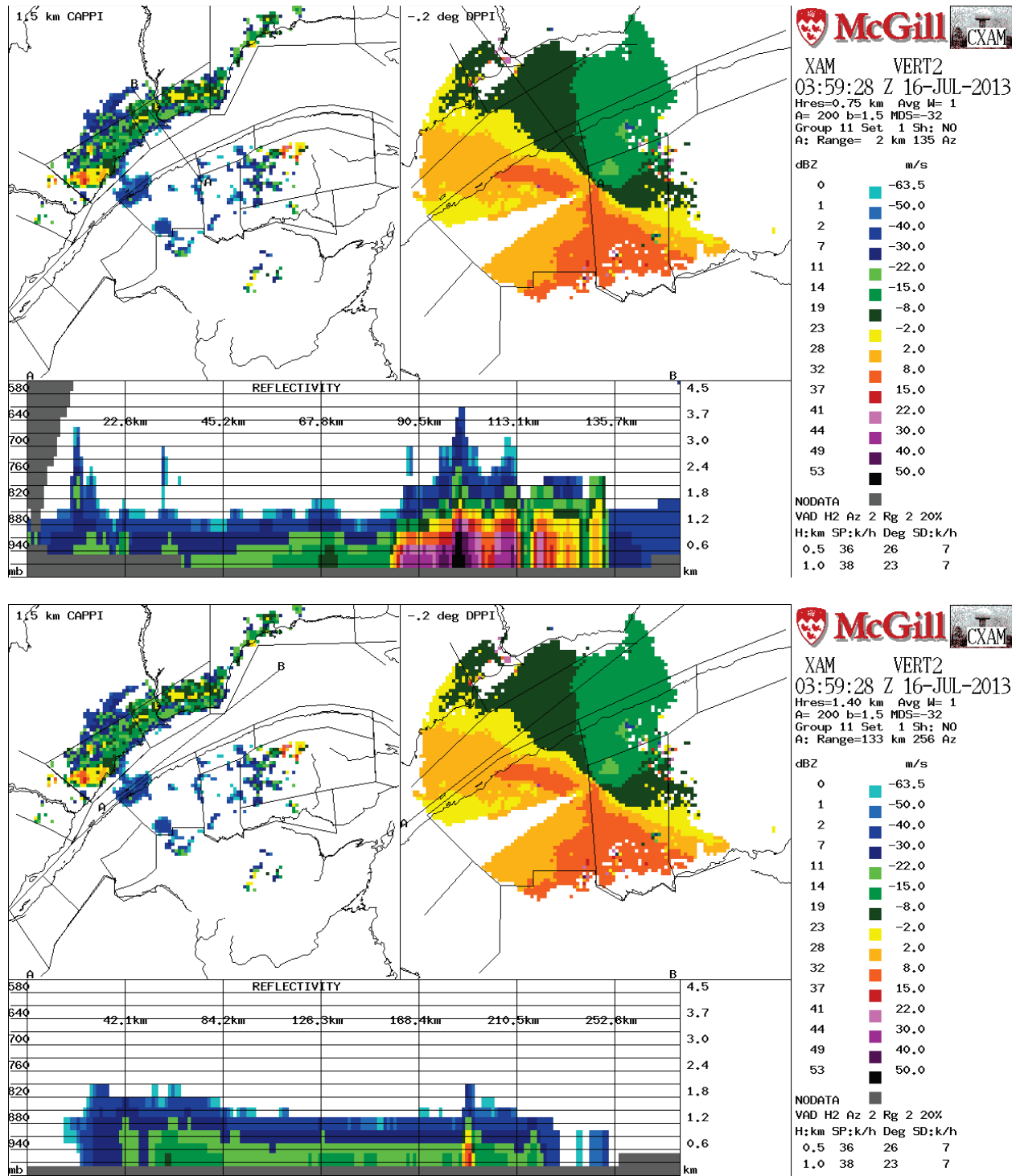


Fig. 11: Vertical cross-sections across the River (top) and along the River (bottom) made at 0:00 EDT. Each figure is made of 3 images, a horizontal section of reflectivity at 1.5 km altitude (upper left), a low-elevation PPI of Doppler velocity (upper right), and the vertical section itself (lower panel) done between the points "A" and "B" shown on the horizontal maps. Vertical sections show both insects (green and blue) as well as ground targets (stronger echoes). These sections illustrate that insects appear to be concentrated in the bottom 500 m of the atmosphere.

The location of the landing of insects could not be easily determined. There is no evidence of massive landing of moths prior to 06:00 UTC (2:00 EDT), and the radar data are ambiguous after. Only around dawn is it clear that all insects that are not over the St-Lawrence are landing while those still over the Gulf remain airborne until they are west of Forestville at which point they are far enough from Val d'Irène to literally fly under the radar. What we can nevertheless say is that the moths were moving SSE ahead of the front, and then SW afterwards, at speeds between 45 km/hr (earlier in the night) and 35 km/hr (later in the night).

Concluding remarks

The outbreak of 15-16 July 2013 was a spectacular one where, if our calibration calculations are correct, of the order of a hundred billion moths took off from the North Shore and tried to cross the Gulf of Saint-Lawrence. Most never reached the South Shore thanks to a shift in the winds that pushed them back towards the west, while the majority of those that made the crossing landed west of Matane and of areas affected by the moth in Gaspésie.

What we hope that this analysis illustrates is the value of radar both for monitoring moth dispersion as well as evaluating dispersion models.

Appendix A: A target recognition approach

Excerpts from Fabry (2015), Chapter 4

Given the long list of observable targets, their proper identification may appear to be a daunting task, especially since there can be considerable overlap between the characteristics of different types of echoes. Therefore, there is no easy step-by-step method to determine target type. A good approach is to look at the structure and behavior of the echo, and determine whether these fit what would be expected for different types of targets. At the end, most types of targets will be eliminated, and hopefully one type of echo will be found to be the most probable.

Characteristics that should be considered include:

- a. Echo strength: What is the average and peak strength of the echo? Near the surface, within the first 2 km, most targets are possible but many have typical echo strength ranges. At usual weather radar wavelengths, strong echoes (> 40 dBZ) are from convective precipitation, the strongest (> 60 dBZ) being generally associated with hail. Moderate echoes (25–40 dBZ) are generally associated with strong widespread precipitation, but widespread precipitation can have intensities down to below 0 dBZ if it comes from drizzle. Echoes from ash and chaff also have similar intensities. Echoes weaker than 25 dBZ can come from many types of targets, though those from liquid clouds and refractive index gradients are improbable above -10 dBZ. Note that ground targets can have any intensity and therefore fit in all those categories;
- b. Size and shape: Targets have a variety of shapes, some of which leading to characteristic echo patterns. Globular echo patterns (Figs. A.1 right, A.5 top, and A.9 right), arranged in clusters or lines of tens to a few hundreds of kilometers, especially if they move, are from precipitation, generally convective. If echoes are more extended and with less structure (Figs. A.1 left and A.9 left), especially if they extend above 3 km, are also from precipitation, generally stratiform. When they are elongated along an axis that is not on a radar radial, they can be from chaff (Fig. A.18) or from interference if they form an extremely thin line (Fig. A.19). When elongated along a radial, echoes could also be from a hail spike (only if the echo pattern is short and located immediately behind a very strong target, Fig. A.12), or interference from another source (if it is very thin, extends at all ranges, and remains on the same azimuth with time, Fig. A.17). Point targets could be from unedited noise if the reflectivity is weak or from airplanes or isolated birds if the echo is stronger. Note that the perceived size and shape is also affected by the geometry of radar measurements because the altitude of observation and radar sensitivity change with range. As a result, weak or low-level targets whose concentration near the surface is nearly uniform will often appear as disks centered on the radar (Fig. A.16); this will be the case for birds, insects, sea clutter, and weak stratiform precipitation. Another example is the bright band that will often be detected as a sometimes-incomplete ring centered on the radar on PPIs at sufficiently high elevation;
- c. Vertical structure: Echoes extending from the surface to above 3 km are generally from precipitation, ash and chaff remaining a possibility. Within these, the presence of a bright band at an altitude where the 0°C would be expected is a clear signature of precipitation that melted from snow to

rain. If the bright band is absent, snow or warm rain is being observed, unless the echo is very strong in which case convective storms are present. Echoes whose intensity decreases rapidly with height from the surface could still have many origins. Strong echoes decreasing very rapidly with height are generally from clutter. Weaker echoes extending to a few kilometers can still be drizzle, snow, insects, or birds. Unusual patterns such as echoes limited to one PPI are unlikely to be of meteorological origin and are often caused by interference or the sun;

d. Movement: Movement is a useful clue especially for targets that are not horizontally uniform. This is because weak echoes that have little horizontal structure will appear to be stationary even if they move: the combination of the lack of patterns to track and the inability of radar to detect weak targets beyond a certain range leads to an echo with the disk shape mentioned above that appears to stay fixed around the radar. An echo pattern that stays absolutely stationary for an extended period (more than two hours), especially if it has a lot of small scale structure, is probably from clutter. Echoes that evolve but seem locked in position could be from precipitation that keeps reforming on topography, but are often associated with ash released by a fire or an eruption;

e. External clues: Other data sources can occasionally provide key missing information. In particular, the absence of clouds on satellite imagery rules out all weather targets except for very weak clear air echoes. Temperature is also important to consider: snow is unlikely above 0°C, while birds and insects are unlikely below 0°C; drizzle and rain are also rare below -10°C;

f. Likelihood: When echo characteristics are insufficient to determine the nature of the target, and external clues are ambiguous, using the likelihood of occurrence remains the best approach. Echoes from precipitation are common, and so are ground targets, especially in the absence of clutter filtering. Over land, insect echoes are common when temperatures are warm enough while over oceans, sea clutter occurs regularly at close range if the winds are strong enough. Migrating birds are regularly observed on spring and fall nights, especially if winds are favorable, but not at other times. Interference echoes may or may not be common, depending on the area and the radar frequency. Ash and chaff are generally rare, the occurrence of the latter being a function of how close the radar is located to an air force base.

Even with these tests, there may remain ambiguities, particularly for weaker echoes at low altitudes, and more information is needed. This is where other radar measurements such as Doppler velocity and those derived from multiple polarizations will help.

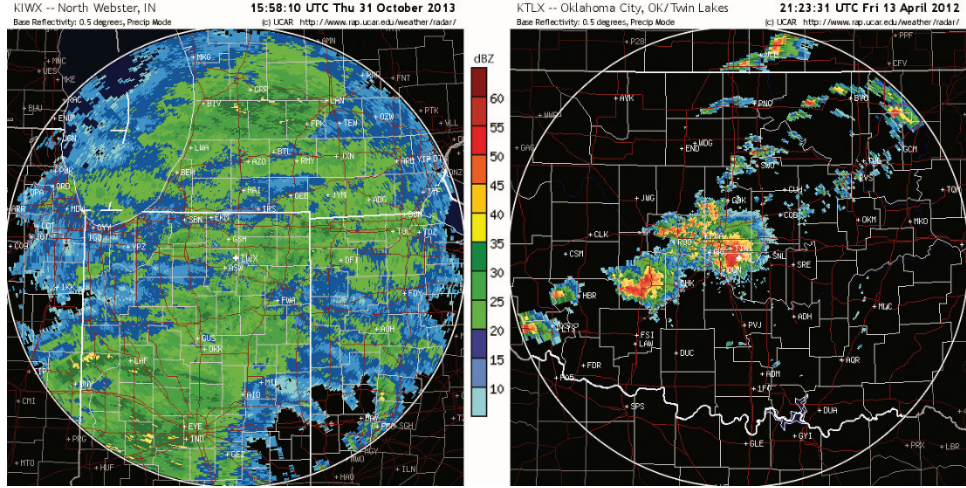


Figure A.1. Low-level PPIs of equivalent radar reflectivity factor (left) of a low-pressure system driven by baroclinic instability and (right) of thunderstorm cells generated by convective instability. The outer ring is 230 km from the radar.

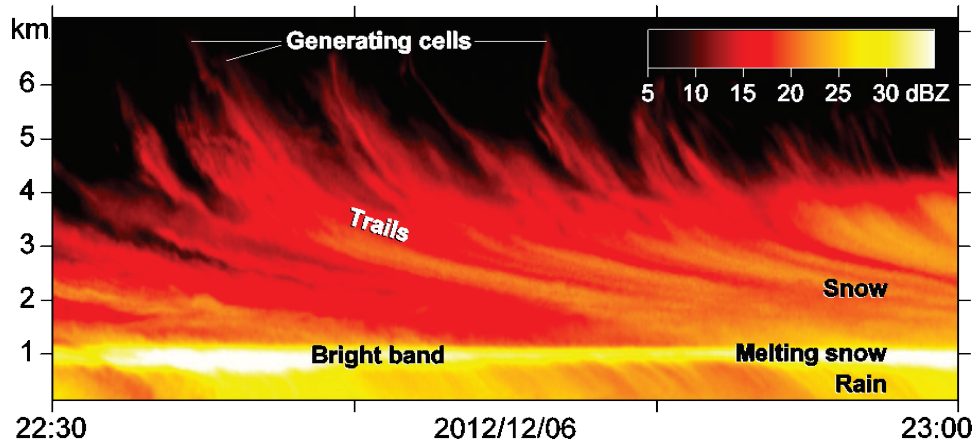


Figure A.5. Annotated time-height section of reflectivity in large-scale precipitation.

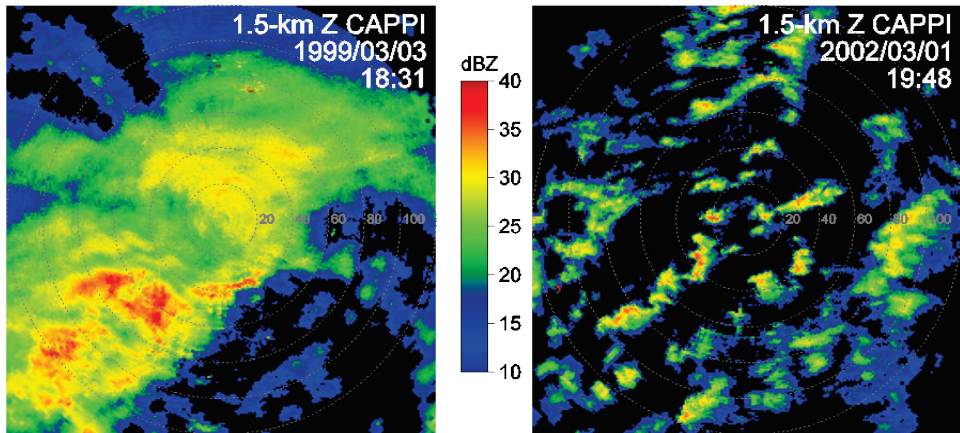


Figure A.9. Reflectivity CAPPIs at an altitude of 1.5 km in widespread snow ahead of an approaching low pressure system (left) and in showery snow behind a cold front (right). Range rings are 20 km apart.

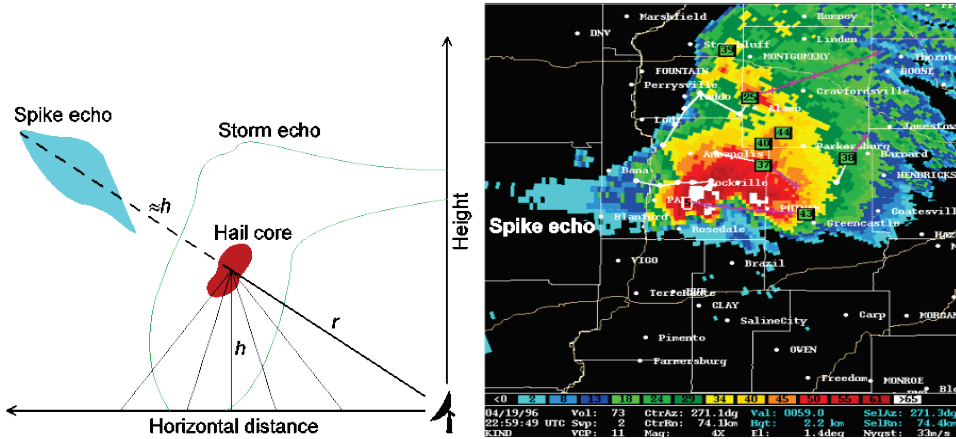


Figure A.12. Left: Conceptual diagram illustrating how the hail spike echo forms as a result of the reflection of strong hail returns first directed towards the surface, then back to the hail core and then to the radar (adapted from Wilson and Reum 1988). Right: Example from the Indianapolis WSR-88D radar; the radar is located right of the image.

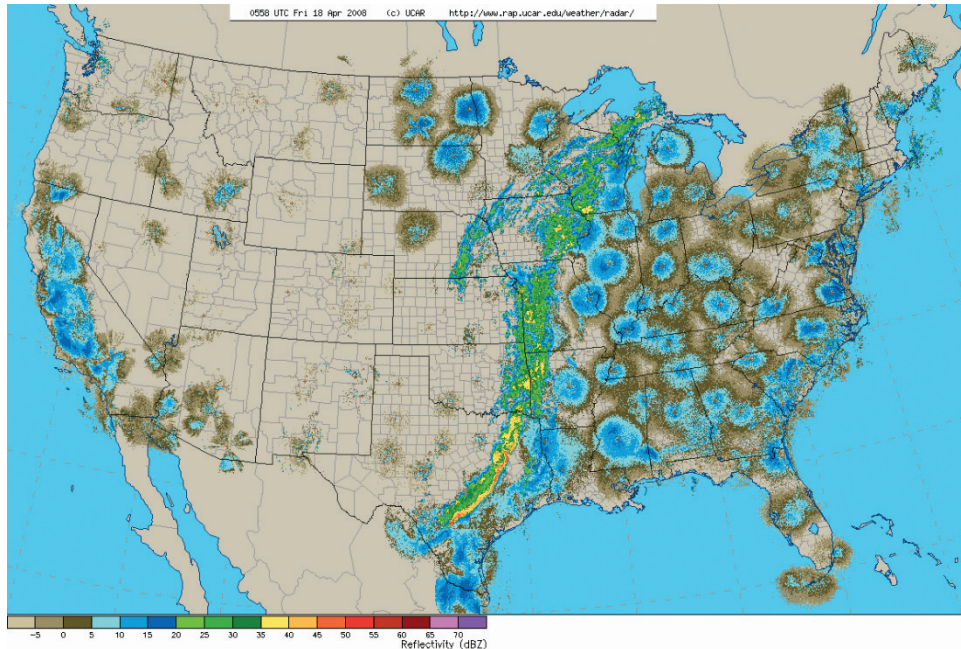


Figure A.16. Composite of reflectivity information from all US radars on the night of 17-18 April 2008 (2:00 EDT in the east, 23:00 PDT in the west). One can observe near the center of the continent a relatively strong band of echoes from precipitation associated with a low pressure system. East of it, disks of weaker echoes caused by bird migration can be seen around almost all radars. In spring, birds migrate primarily ahead of approaching storms where they can benefit from southerly tail winds but not when winds blow in the opposite direction as is the case west of the storm. The reverse is true in fall. Birds may be bird-brained, but they are not stupid!

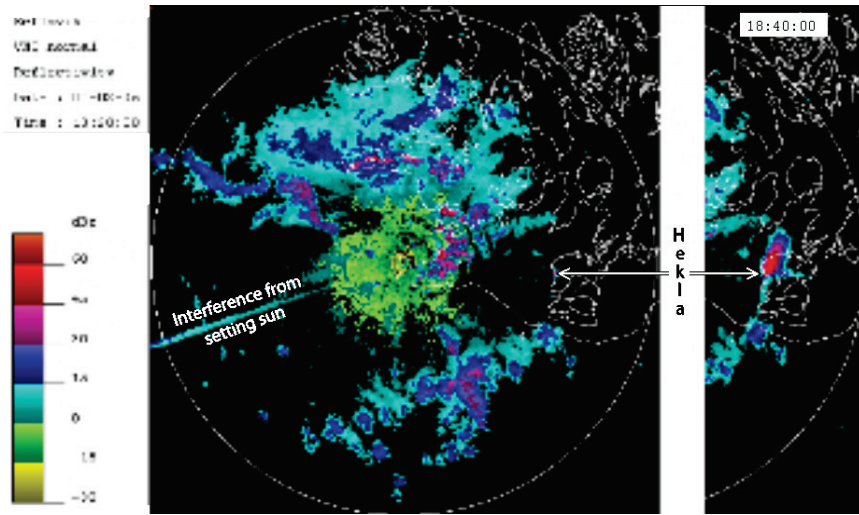


Figure A.17. Map of maximum intensity in the vertical from the Keflavik radar in Iceland two minutes (left) and twenty-two minutes (right) after the beginning of the eruption of the Hekla volcano on 26 February 2000. The location of the Hekla is indicated. Other echoes visible in the two maps include ground and sea clutter at close range, two broad regions of precipitation to the north and south, and interference from the setting sun (along with visible light, the sun emits weakly in the microwaves; when the radar points at the sun, these emissions are detected by the radar and can be wrongly interpreted as "echoes"; other sources such as local area networks (LAN) may give similar signatures). Adapted from Lacasse et al. (2004).

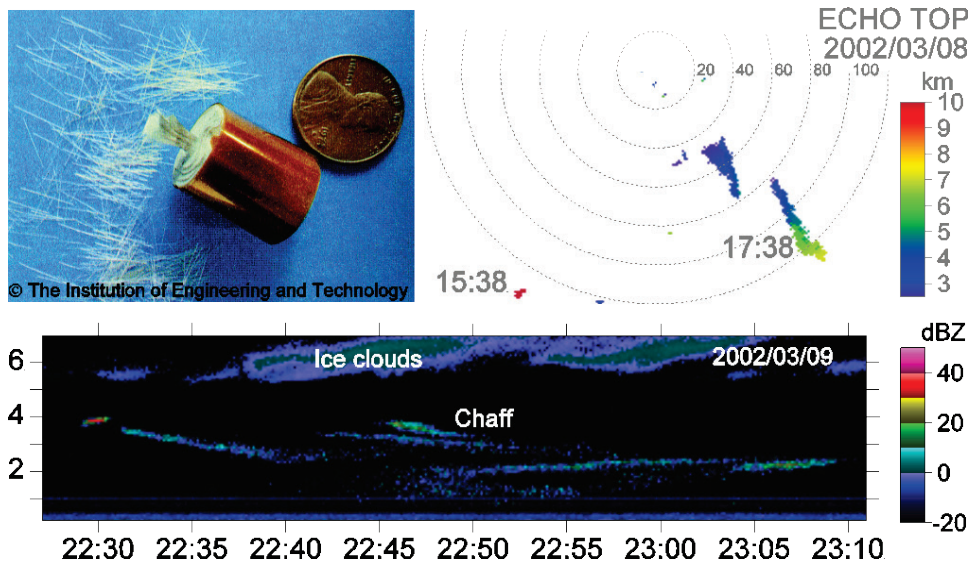


Figure A.18. Top left: Picture of a small cylindric container full of chaff fibers, some of which have been pulled out (Stimson 1998). Top right: Echo-top map showing chaff soon after its release when it still forms a strong point-like target (15:38), and two hours later (17:38) when it has taken the shape of a descending trail because of the different fall speeds of each fiber. Bottom: Height-time section of reflectivity of chaff echoes from another release.

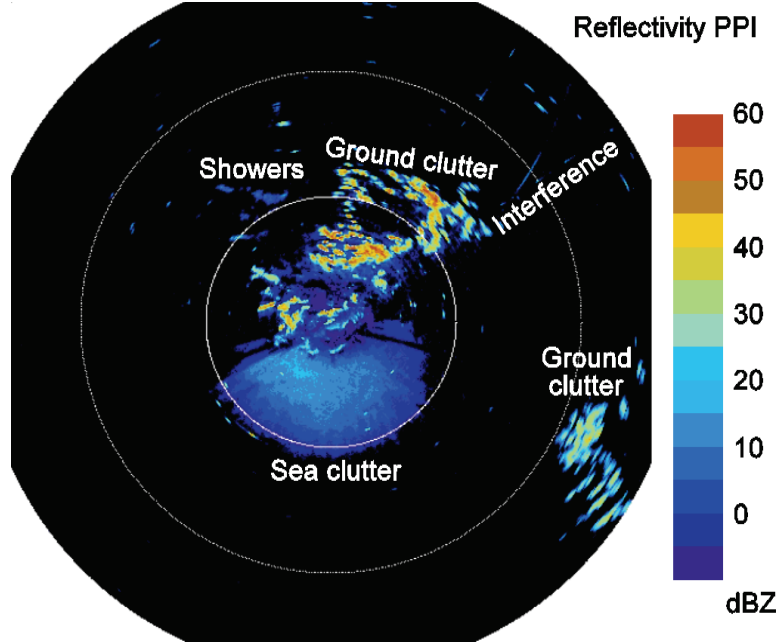


Figure A.19. Example of a variety of unwanted clutter echoes observed by the French Collobri  re radar near the Mediterranean Sea. Among a few small shower echoes to the north-west, one can observe echoes from ground targets (strong textured echoes or small arcs along a fixed range), from the sea surface (the lighter more uniform area to the south), and interference from other radar transmitters (short segments along an azimuth or the SW-NE oriented arc over the “terfe” of “interference” on the image. Range rings are every 60 km. Original image courtesy of P. Tabary.

Appendix B: Estimating moth density by weather radars

To estimate the density of moths by weather radars, we have to go back to basic principles of scattering of radio waves by simple targets and apply this theory for moths and weather radars. While there are rigorous ways to compute the reflectivity of a target knowing its shape and material properties, we chose here to use a first-order estimation approach to rapidly get an approximate value given the complexity of the shape of moths and the variability in their size and mass.

Weather radars in North America have a wavelength of either 5.5 cm (Environment Canada radars) or 10.5 cm (McGill and U.S. radars). For targets much smaller than the wavelength, which is (barely) the case of SBW moths, the amount of power reflectivity goes as the sixth power of the equivalent target diameter D^6 , a 2-mm target reflecting 2^6 or 64 times more than a 1-mm target. Weather radars are calibrated to estimate the equivalent radar reflectivity of water drops in $\text{mm}^6 \text{ m}^{-3}$, one 1-mm drop per cubic meter giving a reflectivity Z of $1 \text{ mm}^6 \text{ m}^{-3}$ while three 2-mm drops per cubic meter gives a reflectivity Z of 3×2^6 or $192 \text{ mm}^6 \text{ m}^{-3}$. Because reflectivity spans a large range of numbers, it is generally reported in dBZ units, where $\text{dBZ} = 10 \log_{10}(Z)$. Using the previous example, our 1-mm drop per cubic meter would give a reflectivity of 0 dBZ ($10 \log_{10}(1) = 0$) while the three 2-mm drops per cubic meter would give a reflectivity of 22.8 dBZ ($10 \log_{10}(192) = 22.8$).

For randomly oriented insects, Riley (1985) found that insects in general reflect like water drops of similar mass (Riley 1985). A typical female spruce budworm (SBW) moth weighs of the order of 12 mg (Thomas et al. 1980), the weight of a 2.84 mm drop. If that was the case, the reflectivity of one female SBW moth per cubic kilometer would be $(2.84 \text{ mm})^6 / (1000 \text{ km/m})^3$ or $5.25 \times 10^{-7} \text{ mm}^6 \text{ m}^{-3}$, or -63 dBZ.

Two corrections must be applied to this estimation to take into account the non-spherical shape of moths and the geometry of radar observations. Moths can be assimilated to prolate spheroids (more or less the shape of an American football) with their long axis (10.6 mm for female moths (de Granpré, 2015, personal communication)) about 3.3 times larger than their other dimensions (width and height of 3.2 mm for female moths, de Granpré, 2015, personal communication). They are also oriented horizontally, with the radar makes measurements at horizontal polarization. Both effects will increase the reflectivity of individual moths compared to the Riley (1985) approximation used above. We are unable to make good calculations of the two effects. More rigorous calculations for a 3:1 axis ratio for birds (higher density than insects) by Vivekanandan et al. (2013) lead to a 14 dB enhancement; in our case, because insects have a smaller density, we expect that enhancement to be reduced to approximately 5 dB (we intend to perform a more thorough calculation later). Hence, we expect the reflectivity of a single female SBW moth per cubic kilometer to be around -58 dBZ. We also estimate the uncertainty on this estimation to be of order of a factor 2, or 3 dB.

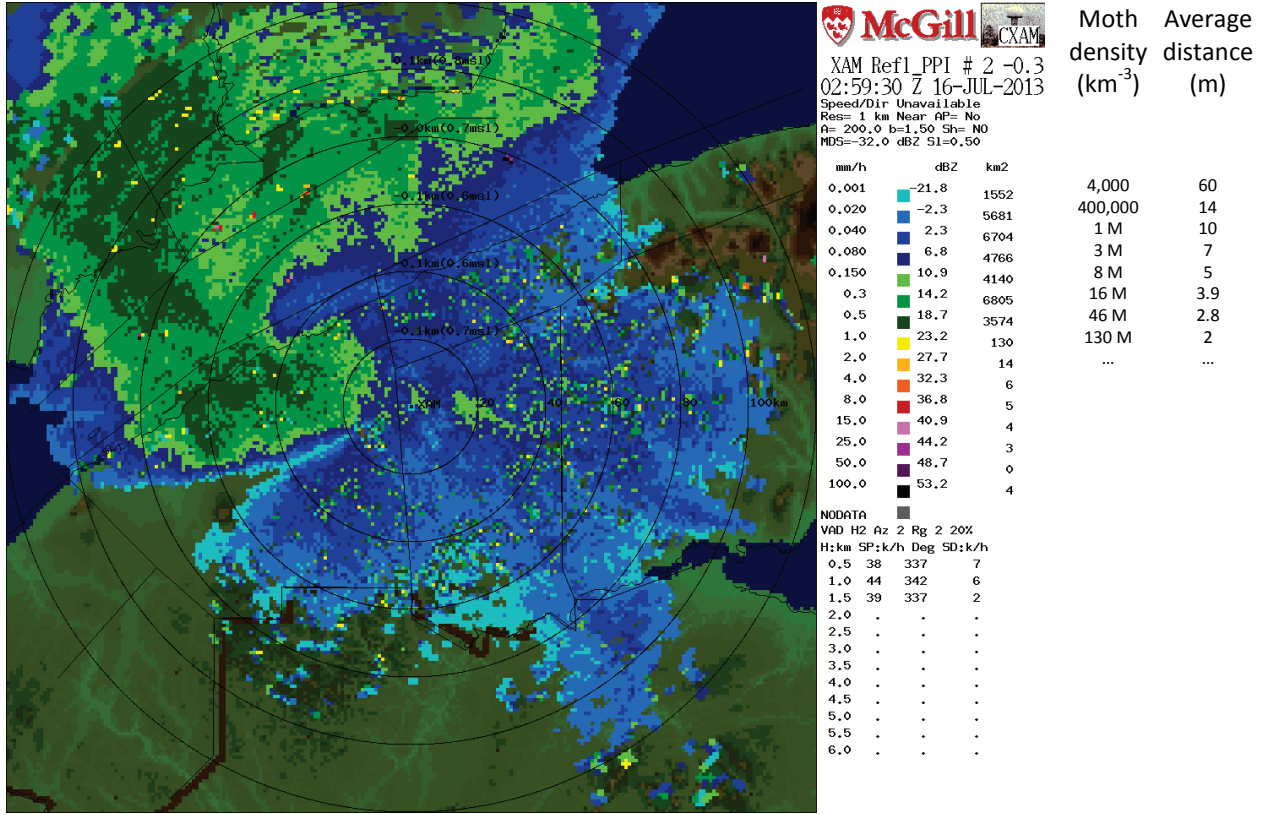


Fig. B.1: Reflectivity from the insect product from the Val d'Irène radar near the peak of the dispersal at 3:00 UTC (23:00 EDT). Next to the reflectivity scale (dBZ) and the area over which a specific reflectivity interval is observed (km^2) are added the expected moth density (assuming females) averaged over the radar beam (in numbers per km^3) for each reflectivity value on the scale and the corresponding average distance between moths in meters.

This benchmark can then be used to attempt to estimate moth density. For example, a reflectivity of 11 dBZ as was observed at low elevation angles during peak dispersal (Fig. B.1) would imply a density of female moths of $10^{(11/10)} / 10^{(-58/10)} = 10^{6.9} \text{ km}^{-3}$ or eight million moths per cubic kilometer. Given a uniform distribution within the volume sampled by the radar, eight million moths per cubic kilometer would translate to an average distance between moths of $[(10^{6.9} \text{ km}^{-3})^{1/3} / 10^3 \text{ m km}^{-1}]$ or five meters. While the result appears to be spectacular, we must acknowledge the fact that this event was chosen because it was one of the most spectacular dispersal events identified on radar.

Appendix C: Datasets and images provided

In addition to this document, a variety of images and datasets were provided to Yan Boulanger. These include:

- 1) Images (PNG format) of the filtered reflectivity for the entire sequence of 15-16 July 2013;
- 2) Two sets of images of the two vertical profiles of reflectivity at 4:00 UTC, one set at high sensitivity that unfortunately enhances weak clutter spreading to high levels, and one with the weaker reflectivity truncated to minimize confusion (Fig. 11);
- 3) Data files of the filtered reflectivity product. The data files contain the reflectivity measured at each point of a 240×240 array of 1×1 km pixels in Cartesian coordinates centered on the Val d'Irène radar. It is a text file where each line contains the latitude, longitude, and reflectivity information for each pixel. For example, the first few lines in the file cleaned_ref_ppi_xam_201307160329_1km.csv are:

```
latitude,longitude,reflectivity
49.543,-69.255,-99.0
49.543,-69.242,-99.0
49.543,-69.228,-99.0
49.543,-69.214,-99.0
49.544,-69.200,-99.0
49.544,-69.186,-99.0
49.544,-69.172,-99.0
49.544,-69.159,-99.0
49.544,-69.145, 3.5
49.545,-69.131, 3.5
49.545,-69.117, 3.5
49.545,-69.103, 5.5
49.545,-69.089, 5.5
49.545,-69.076, 5.5
49.545,-69.062, 4.0
49.546,-69.048, 4.0
49.546,-69.034, 4.0
49.546,-69.020, 7.0
49.546,-69.006, 6.0
49.546,-68.992, 6.0
49.546,-68.979, 10.5
49.547,-68.965, 8.5
49.547,-68.951, 8.5
```

The first 2 fields in each line are the latitude and longitude of the pixel and the third field is the cleaned reflectivity in dBZ. A value of -99.0 indicates that there was no detectable for that pixel. Other numbers whether smaller than, equal, or greater than 0 are valid reflectivity values. The name of the file contains the date and time stamp of the product together with the 3 letter code name of the radar (xam) and pixel resolution (1 km), e.g., cleaned_ref_ppi_xam_201307160329_1km.csv. These files can be read and viewed by Excel or other spreadsheet programs that can read comma-separated variable (csv) files.

References

- Fabry, F., 2015: *Weather Radars, Principles and Practice*. Cambridge University Press.
- Riley, J. R., 1985: Radar cross section of insects. *Proceedings of the IEEE*, **73**, 228–232.
- Thomas, A. W., S. A. Borland and D. O. Greenbank, 1980. Field fecundity of the spruce budworm (Lepidoptera: Tortricidae) as determined from regression relationships between egg complement, fore wing length, and body weight. *Canadian Journal of Zoology*, **58**, 1608–1611.
- Vivekanandan, J., J. Hubbert, S. Ellis and J. Wilson, 2013: Radar observations and radar model computations of biological scatterers. *Preprints*, 36th Conf. on Radar Meteorology, Breckenridge, CO, Amer. Meteor. Soc., paper 13A.1.